Entanglement generation in persistent current qubits

J.F. Ralph[1], T.D. Clark[2], T.P. Spiller, W.J. Munro
Trusted Systems Laboratory
HP Laboratories Bristol
HPL-2004-110
June 30, 2004*

entanglement, quantum information, flux qubit, persistent current qubit

In this paper we investigate the generation of entanglement between two persistent current qubits. The qubits are coupled inductively to each other and to a common bias field, which is used to control the qubit behaviour and is represented schematically by a linear oscillator mode. We consider the use of classical and quantum representations for the qubit control fields and how fluctuations in the control fields tend to suppress entanglement. In particular, we demonstrate how fluctuations in the bias fields affect the entanglement generated between persistent current qubits and may limit the ability to design practical systems.

* Internal Accession Date Only
[1]J.F. Ralph, Department of Electrical Engineering and Electronics, University of Liverpool, Brownlow Hill, Liverpool, L69 3GJ
[2]School of Engineering, University of Sussex, Falmer, Brighton, BN1 9QT Approved for External Publication

Entanglement generation in persistent current qubits

J. F. Ralph,[1,*] T. D. Clark,[2] T. P. Spiller,[3] and W. J. Munro[3]

[1]*Department of Electrical Engineering and Electronics, The University of Liverpool, Brownlow Hill, Liverpool, L69 3GJ, United Kingdom*
[2]*School of Engineering, The University of Sussex, Falmer, Brighton, BN1 9QT, United Kingdom.*
[3]*Hewlett-Packard Laboratories, Filton Road, Stoke Gifford, Bristol BS34 8QZ, United Kingdom*

(Dated: January 12, 2004)

In this paper we investigate the generation of entanglement between two persistent current qubits. The qubits are coupled inductively to each other and to a common bias field, which is used to control the qubit behaviour and is represented schematically by a linear oscillator mode. We consider the use of classical and quantum representations for the qubit control fields and how fluctuations in the control fields tend to suppress entanglement. In particular, we demonstrate how fluctuations in the bias fields affect the entanglement generated between persistent current qubits and may limit the ability to design practical systems.

PACS numbers: 03.65.-w, 74.50.+r, 85.25.Dq

INTRODUCTION

In this paper, we investigate the use of inductive coupling to generate entanglement between two persistent current qubits. We are particularly interested in the representation of the magnetic bias fields that are used to control the behaviour of the qubits, and the requirements placed on these fields by the need to generate significant levels of entanglement. Given the recent experimental results indicating coherent quantum behaviour in superconducting persistent current and other Josephson devices [1–3], the extension of these systems to arrays of coupled qubits for quantum information processing is important and timely. Indeed, experiments have already been reported using coupled persistent current qubits [4]. We demonstrate that the requirements placed on the bias fields could present significant obstacles to the use of persistant current qubits in quantum information processing.

We consider two models for the bias field: one classical and one quantum mechanical. In each model, the field is represented by a lossy linear oscillator, whose resonant frequency and coupling to the qubits can be varied. When the natural frequency of the field mode is significantly lower than the qubit frequencies, the conventional approach is to treat the bias as a classical variable [1–4] and to use the expectation value of the screening current in the classical equations of motion when the bias dynamics are important [5, 6]. However, where the bias field has fluctuations at frequencies that are comparable with the qubit fluctuations, the classical model is no longer valid and the quantum mechanical model predicts some interesting dynamical behaviour. In addition, we derive a set of constraints for the accuracy of the bias fields which must be obeyed for a significant amount of entanglement to be produced. These constraints may limit the entanglement that can be produced in a practical system. In particular, we derive restrictions on the coupling between the qubits and the bias fields and the operating frequencies of multiple persistent current qubits.

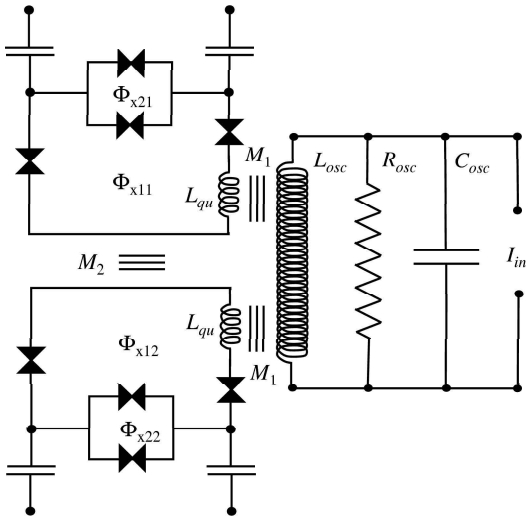

FIG. 1: Schematic diagram of coupled qubit system.

COUPLED PERSISTENT CURRENT QUBITS

The persistent current qubits studied in this paper have been proposed by Orlando et al. [1]. A schematic circuit diagram is given in Figure 1, with inductive coupling between the two qubits and the common control field. The qubit inductance is negligible when compared with the effective inductance generated by the series Josephson junctions in the loop. This means that the behaviour of an isolated qubit will tend to be dominated by the series Josephson junctions rather than the geometrical inductance of the ring, $L_{qu} \simeq 10$ pH. This allows the circuit to be simplified to a two-state model, correspond-

ing to current states differing by approximately 600 nA [1]. The two-state Hamiltonian for a single qubit, with two control fields Φ_{x1} and Φ_{x2}, is given by [1],

$$\hat{H}_{qu}(\Phi_{x1},\Phi_{x2}) = \begin{pmatrix} F(\Phi_{x1},\Phi_{x2}) & -B(\Phi_{x1},\Phi_{x2}) \\ -B(\Phi_{x1},\Phi_{x2}) & -F(\Phi_{x1},\Phi_{x2}) \end{pmatrix} \tag{1}$$

where the basis states, $\{|0\rangle,|1\rangle\}$, are the persistent current states with approximately ± 300 nA, Φ_{x1} is the primary bias field for the main ring circuit and Φ_{x2} is a secondary bias field that is used to modulate the critical current of the effective Josephson junction formed by the two parallel junctions in the smaller secondary ring. The matrix elements are given by,

$$F(\Phi_{x1},\Phi_{x2}) = r_1\left(\frac{\Phi_{x1}}{\Phi_0}\right) + r_2\left(\frac{\Phi_{x2}}{\Phi_0}\right) \tag{2}$$

$$B(\Phi_{x1},\Phi_{x2}) = \frac{t_1 + s_1\left(\frac{\Phi_{x1}}{\Phi_0}\right)}{1-\eta\sqrt{\frac{E_J}{E_C}}\left(\frac{\Phi_{x2}}{\Phi_0}\right)} \tag{3}$$

and $\Phi_0 = h/2e = 2\times 10^{-15}$ Wb. The circuit constants are taken from [1]: $r_1 = 2\pi E_J\sqrt{1-\frac{1}{4\beta^2}} = 2r_2$, $s_1 = 0$, $t_1 = 0.001E_J$, $\eta = 3.5$, $\beta = 0.8$, $E_J \equiv 200$ GHz, $E_C = E_J/80$.

Although the energy level separation, and hence the dynamics of a single persistent current qubit, is dominated by the Josephson energy of the junctions in the circuit, the inductance is important when determining the coupling between the qubit and the external fields and between the qubits themselves. For the system shown in Figure 1, this gives

$$\begin{aligned} \begin{pmatrix} \Phi_{qu_1} \\ \Phi_{osc} \\ \Phi_{qu_2} \end{pmatrix} &= \begin{pmatrix} L_{qu} & M_1 & M_2 \\ M_1 & L_{osc} & M_1 \\ M_2 & M_1 & L_{qu} \end{pmatrix} \begin{pmatrix} I_{qu_1} \\ I_{osc} \\ I_{qu_2} \end{pmatrix} \\ &= \mathbf{M}\cdot\begin{pmatrix} I_{qu_1} \\ I_{osc} \\ I_{qu_2} \end{pmatrix} \end{aligned} \tag{4}$$

where M_1 is the mutual inductance between the qubits and the bias coil and M_2 is the mutual inductance between the two qubits, Φ_{osc} is the magnetic flux in the shared bias field (which is treated as a linear oscillator and characterized by a capacitance C_{osc} and an inductance L_{osc}). In the absence of dissipation, the effective Hamiltonian for the combined system can be written in the form [5],

$$\begin{aligned} H &= \frac{Q_{osc}^2}{2C_{osc}} + \frac{\Phi_{osc}^2}{2L_{osc}} - \Phi_{osc}I_{in} \\ &\quad + \hat{H}_{qu_{1+2}}(\mu_1\Phi_{osc},\Phi_{x21};\mu_1\Phi_{osc},\Phi_{x22}) \end{aligned} \tag{5}$$

where I_{in} is an external current used to fix the static bias point (the oscillator fluctuates about this point), and the coupling coefficients are given by $K_1^2 = M_1^2/L_{qu}L_{osc}$, $\mu_1 = M_1/L_{osc}$ and $K_2^2 = M_2^2/L_{qu}^2 = \mu_2^2$. Each qubit has two bias/control fields, Φ_{x11} and Φ_{x21} for qubit 1 and Φ_{x12} and Φ_{x22} for qubit 2. The primary control fields for the qubits, Φ_{x11} and Φ_{x12}, are common so we put $\Phi_{x11} = \Phi_{x21} = \mu_1\Phi_{osc}$.

To derive the Hamiltonian for the two qubits, we examine the energy of the inductive circuit components. The Hamiltonian terms corresponding to the inductive energies will have the form,

$$\begin{aligned} H_{induc} &= \frac{1}{2}(\Phi_{qu_1}\ \ \Phi_{osc}\ \ \Phi_{qu_2})\cdot\mathbf{M}^{-1}\cdot\begin{pmatrix}\Phi_{qu_1}\\ \Phi_{osc}\\ \Phi_{qu_2}\end{pmatrix} \\ &= \frac{1}{2}(I_{qu_1}\ \ I_{osc}\ \ I_{qu_2})\cdot\mathbf{M}^{T}\cdot\begin{pmatrix}I_{qu_1}\\ I_{osc}\\ I_{qu_2}\end{pmatrix} \end{aligned} \tag{6}$$

Expanding the second of these expressions, the cross-coupling terms between the two qubits has the form: $\Delta H_{qu_{1+2}} = \mu_2 L_{qu}\hat{I}_{qu_1}\hat{I}_{qu_2}$. The other terms corresponding to a shift in the effective self inductance of the qubits and cross-coupling between the qubits and the oscillator are subsumed into the F and B terms. The two qubit Hamiltonian then has the form,

$$\hat{H}_{qu_{1+2}}(\Phi_{x11},\Phi_{x21};\Phi_{x12},\Phi_{x22}) =$$

$$\begin{pmatrix} F_1+F_2+\Delta_{12} & -B_2 & -B_1 & 0 \\ -B_2 & F_1-F_2-\Delta_{12} & 0 & -B_1 \\ -B_1 & 0 & -F_1+F_2-\Delta_{12} & -B_2 \\ 0 & -B_1 & -B_2 & -F_1-F_2+\Delta_{12} \end{pmatrix} \tag{7}$$

in the current basis $\{|0_1 0_2\rangle, |0_1 1_2\rangle, |1_1 0_2\rangle, |1_1 1_2\rangle\}$ (which is used as the computational basis for the purposes of this paper), and where $F_1 = F(\Phi_{x11},\Phi_{x21})$, $B_1 = B(\Phi_{x11},\Phi_{x21})$, $F_2 = F(\Phi_{x12},\Phi_{x22})$, $B_2 = B(\Phi_{x12},\Phi_{x22})$. The Δ term comes from the qubit-qubit coupling term given in equation (6), with $\Delta_{12} = K_2 L_{qu}\bar{I}_{qu}^2$, where $\bar{I}_{qu} \simeq 300$ nA is the magnitude of the screening current in the qubit logic (persistent current) states.

We assume that both qubits are identical and we consider the dynamics of a (common) primary control field Φ_{osc}, keeping the secondary fields Φ_{x21} and Φ_{x22} fixed. Both the primary and secondary fields are nominally set to zero so that the energy eigenstates of the individual qubits are symmetric/anti-symmetric superpositions of the qubit current states. Initialising the qubits in a current state will produce coherent oscillations at frequencies around 400 MHz. Although the fields are nominally zero, they all include a fixed error and the primary field includes the dynamics of the bias circuit. (We use a common primary bias for computational simplicity and because the decoherence rate will be lower where any noise due to the flux bias is the same for each qubit).

For simplicity, we assume that the couplings are weak, typically $K_1 = 0.002$ and $K_2 = 0.01$. This means that first order coupling terms will be sufficient for most purposes. Allowing stronger couplings between the qubits

and the bias fields could introduce a range of problems: difficulties initialising the qubits in a given state since the flux and current states are no longer identical (due cross-couplings in equation (1)), and the quantum fluctuations in the bias coil can affect the ability to generate entanglement (see below).

BIAS FIELDS AND DYNAMICS

We consider two models: one where the control field is a noisy classical field and one where it is represented by a quantum oscillator. The classical oscillator model [5, 6] is expected to be valid as long as (i) the typical frequency of the oscillator is significantly lower than that of qubits, (ii) the (possibly entangled) two-qubit state and the oscillator state are separable, and (iii) as long as the quantum fluctuations of an equivalent quantum oscillator (approximately given by the width of the energy eigenstates in a magnetic flux basis) are small compared to the other fluctuations that couple to the qubits. The quantum model uses a standard harmonic oscillator basis for the control field, and couples via an oscillator flux operator (formed from the raising and lowering operators, $\hat{a}^\dagger$ and $\hat{a}$) in the F and B functions.

The classical approximation is based on the Born-Oppenheimer approximation that is often used in nuclear and molecular physics. This removes the dynamics of a 'fast' degree of freedom by replacing the quantum mechanical operators with their expectation values; thereby averaging or integrating out the effect of their dynamics on the the other 'slow' degrees of freedom. The details of the approximation and the restrictions on its use are more fully described in reference [6]. In this case, the qubit behaviour is assumed to be fast compared to the evolution of the classical oscillator, and the expectation value of the energy is included in the (now classical) Hamiltonian given in equation (5). The classical equation of motion is then derived in the conventional way using the variational derivative with respect to the oscillator magnetic flux Φ_{osc}, and the energy expectation value becomes the expectation value of the combined qubit screening current. Using this approximation, and adding a parallel resistance R_{osc}, the equation of motion is given by [5, 6],

$$\begin{aligned} &C_{osc}\tfrac{d^2\Phi_{osc}}{dt^2} + \tfrac{1}{R_{osc}}\tfrac{d\Phi_{osc}}{dt} + \tfrac{\Phi_{osc}}{L_{osc}} \\ &= I_{in} + \mu_1 \left\langle \hat{I}_{qu_1}(\mu_1\Phi_{osc}, \Phi_{x21}) + \hat{I}_{qu_2}(\mu_1\Phi_{osc}, \Phi_{x22}) \right\rangle \end{aligned} \tag{8}$$

where the qubit screening currents are calculated from the expectation value of the qubit screening current operators $\hat{I}_{qu_1}$ and $\hat{I}_{qu_2}$ over the instantaneous wavefunction (i.e. a pure state) of the two-qubit state (calculated using the time-dependent Schrödinger equation). The time-dependent Schrödinger equation is used for the qubit evolution in this case because, for simplicity, we assume that the dominant source of decohence is the oscillator and any intrinsic dissipation due to emission from the qubits in the cavity is comparatively small. However, the effect of this emssion process on the behaviour of a classical oscillator has been examined elsewhere [7]. The dissipative term acts as a source of classical fluctuations due to Johnson noise in the resistor at finite temperature, taken to be $T = 10$mK which is in line with experimental systems. (The noise need not be thermal, but it is a useful generic model for experimental noise because electronic noise is often characterised in terms of an effective noise 'temperature').

QUANTUM EVOLUTION AND QUANTUM JUMPS

In the quantum model, the reduced density operator for the qubits is estimated using a quantum trajectory model: an unravelling of the Markovian Master equation that produces individual 'trajectories', which can then be averaged over an ensemble to produce an estimate of the density operator [8–10]. (A recent comprehensive review of this subject is given in reference [11]). Each unravelling is equivalent to the Master equation when averaged over an ensemble, but corresponds to a different measurement interaction at the individual system level [10]. For simplicity, we choose the 'quantum jumps' model [8] and thermal environment (Lindblad) operators for the oscillator described in [12],

$$\hat{L}_1 = [(\bar{n}+1)\omega_{osc}Q_{osc}]^{\frac{1}{2}}\hat{a} \qquad \hat{L}_2 = [\bar{n}\omega_{osc}Q_{osc}]^{\frac{1}{2}}\hat{a}^\dagger \tag{9}$$

where $\bar{n} = [\exp(\hbar\omega_{osc}/kT)-1]^{-1}$ is the thermal oscillator occupancy, $\omega_{osc} = 1/\sqrt{C_{osc}L_{osc}}$ is the resonant frequency of the bias feld and the quality factor is given by $Q_{osc} = \omega_{osc}R_{osc}C_{osc}$ (in this paper we use $Q_{osc} = 200$ for both the classical and quantum models). These environmental operators represent emission and absorption of photons from the environment by the oscillator mode, which is assumed to be the dominant source of dissipation in this paper.

The quantum jump evolution is calculated by numerically integrating the full state (describing the qubits and the oscillator) over discrete time intervals (of size dt) and applying three different evolution operators. In each time interval, there is a small (but finite) probability that the bias oscillator will emit or absorb a quantum of energy from the environment. The probabilities for emission and absorption during the time step are found from,

$$P_1(dt) = \left\langle \hat{L}_1^\dagger \hat{L}_1 \right\rangle dt = [(\bar{n}+1)\omega_{osc}Q_{osc}] \left\langle \hat{a}^\dagger\hat{a} \right\rangle dt \tag{10}$$

$$P_2(dt) = \left\langle \hat{L}_2^\dagger \hat{L}_2 \right\rangle dt = [\bar{n}\omega_{osc}Q_{osc}] \left\langle \hat{a}\hat{a}^\dagger \right\rangle dt \tag{11}$$

The jumps are generated stochastically and when a jump occurs, a projection operator is applied to the instantaneous state of the system. If an emission occurs, an operator $\hat{\Omega}_1(dt) = \sqrt{dt}\hat{L}_1$ is applied, lowering the state of the oscillator, and if absorption occurs an operator $\hat{\Omega}_2(dt) = \sqrt{dt}\hat{L}_2$ is applied, raising the oscillator state. The state is then renormalised. In the absence of a quantum jump, the evolution of the system is found from the non-unitary evolution operator,

$$\hat{\Omega}_0(dt) = 1 - \frac{idt}{\hbar}\hat{H} - \frac{dt}{2}(\hat{L}_1^\dagger\hat{L}_1 + \hat{L}_2^\dagger\hat{L}_2) \qquad (12)$$

The non-unitary term is added to ensure that the evolution of the density operator for the coupled system agrees with that predicted by the Markovian Master equation, when the (pure state) density operators generated from an ensemble of individual 'trajectories' are averaged to produce an estimate for the mixed state density matrix for the whole system ρ_{total}: two qubits and bias oscillator. The reduced density operator for the two qubits ρ_{1+2} is then found by performing a partial trace over the oscillator states. (The validity of the quantum jumps approach can be checked by selecting a different unravelling for the Master equation, and in this paper the results have been verified by comparing the behaviour obtained from the quantum jumps unravelling to equivalent results obtained from the quantum state diffusion unravelling [9]. Quantum state diffusion produces a continuous stochastic evolution of the quantum state, and can be shown to correspond to a unit-efficiency heterodyne detection measurement process [10]).

RESULTS

In each model, quantum and classical, the initial conditions set for the oscillator are a thermalised state: a thermal quantum state for the quantum oscillator and an initial condition generated from the classical equation of motion, which has been allowed to come into equilibrium with the thermal noise by numerically integrating its behaviour prior to initialisation using a different realisation of the noise for each qubit trajectory calculation. The qubits are initialised in a product of pure current states. The initial states of the qubits are chosen to be either in-phase ($|0_1 0_2\rangle$) or anti-phase ($|0_1 1_2\rangle$). That is, the coherent oscillations induced by initialising each qubit in a current state are initially in phase with each other or in anti-phase. Each individual quantum trajectory is calculated using the same initial conditions for the qubit states with different static bias errors for the control fields. The static bias errors are fixed for each trajectory and represent the accuracy with which the fields might be set in an experiment. The size of these static bias errors is found to be crucial to the generation of useable entangement between the qubits. The entanglement is characterised in terms of the *concurrence*, which is widely used in quantum information processing for bipartite systems [13]. The concurrence for the two-qubit mixed state density matrix ρ_{1+2} is defined as

$$C(\rho_{1+2}) = max\{0, \sqrt{\lambda_1} - \sqrt{\lambda_2} - \sqrt{\lambda_3} - \sqrt{\lambda_4}\}$$

where $\sqrt{\lambda_1}, \ldots, \sqrt{\lambda_4}$ are the eigenvalues of the matrix $\rho_{1+2}(\sigma_y \otimes \sigma_y)\rho^*_{1+2}(\sigma_y \otimes \sigma_y)$ in nondecreasing order and σ_y is a Pauli spin matrix [14]. Although the concurrence is used here, other measures of entanglement can be calculated from this: e.g. the entanglement of formation E_F can be calculated from

$$E_F(\rho_{1+2}) = h\left(\frac{1}{2}[1 + \sqrt{1 - C(\rho_{1+2})^2}]\right)$$

where

$$h(x) = -x\log_2 x - (1-x)\log_2(1-x)$$

at least for this two-qubit system. The *mixedness* of the resultant two-qubit state is given by the von Neumann entropy of the reduced density operator [14]: $S(\rho_{1+2}) = Tr(\rho_{1+2}\log_4\rho_{1+2})$. The logarithm is taken to base 4 because the qubit states exist in a four-dimensional Hilbert space, giving a mixedness parameter that varies between zero and one.

Figure 2 shows the concurrence of the two-qubit mixed states for bias errors of $\Delta\Phi_x = 10^{-5}\Phi_0$ (1 σ, Gaussian) for both models for an oscillator frequency of 100 MHz. We see that the concurrence oscillates and decays gradually in time, mainly due to dephasing between the two qubits originating from the static error in the bias fields, and approaches a maximially entangled mixed state in each oscillation. By varying the size of the errors, we find that the concurrence is quite sensitive to errors in the static fields, bias errors larger than about $5 \times 10^{-5}\Phi_0$ do not lead to any useful entanglement in the qubits - the concurrence is less than 0.3 at all times and decays very rapidly. (Other calculations away from the minimum splitting point of the qubits, where the frequency differences between energy eigenstates are higher, indicate that the requirements on the bias fields are even more demanding. Where the qubit frequencies are around 1-2 GHz, useful entanglement is only generated if the bias errors are less than about $\Delta\Phi_x \sim 10^{-6}\Phi_0$).

By increasing the couplings between the two qubits, the rate at which the two qubits become entangled can be increased. However, this could lead to problems when initialising the qubit states since the qubit current and flux are mixed by the inductive coupling. Care is required to ensure that the initialisation process projects the states onto the correct basis. (Slight differences in the initial states will affect the entanglement in the mixed state, but this is not explicitly considered here). Increasing the coupling between the oscillator and the qubits is likely to

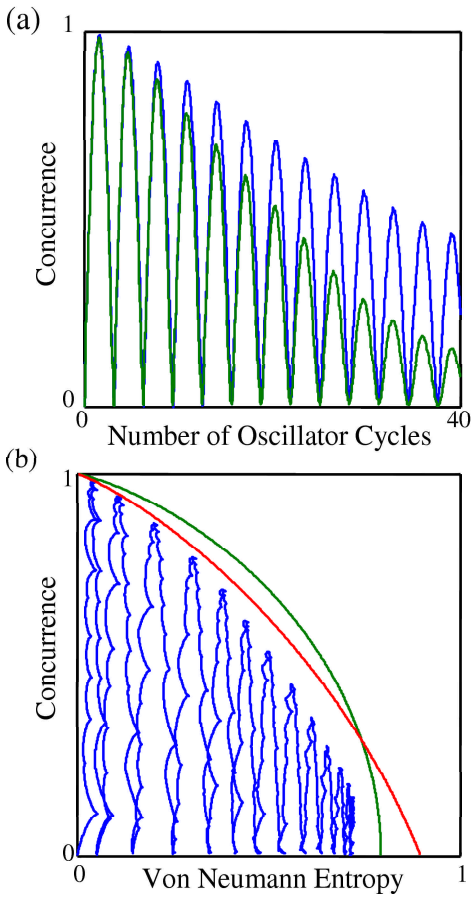

FIG. 2: (a) Concurrence versus number of oscillator cycles (100MHz) for both the classical (blue) and quantum (green) field models, (b) Concurrence versus von Neumann entropy for mixed state (blue) corresponding to the quantum model shown in (a), with two types of maximally entangled mixed states (Rank 3 (green) and Werner states (red) [14]).

lead to additional problems. Although the classical oscillator model contains noise due to thermal fluctuations and dissipation from the finite quality factor of the oscillator, a quantum oscillator also includes quantum fluctuations. The differences in Figure 2(a) for the quantum and classical oscillator models are due to the comparatively low Q value used and the quantum fluctuations coupling across to the qubits. Increasing the oscillator Q and/or reducing the oscillator frequency improves the agreement between classical and quantum models. The coupling between the bias and the qubits is sufficiently small for the entanglement between the oscillator and qubits to be negligible.

This raises an interesting point: what happens when the quantum fluctuations in the oscillator coupling across to the qubits are comparable with the static bias errors? The size of the quantum fluctuations in the oscillator can be estimated from the flux width of the harmonic

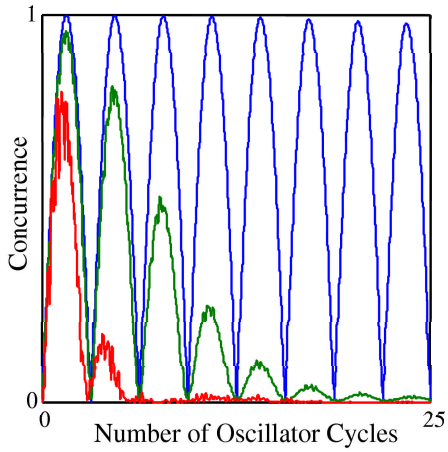

FIG. 3: Concurrence versus number of oscillator cycles (100MHz) for quantum field model with different coupling strengths in the absence of static bias errors: $K_1 = 0.001$ (blue), $K_1 = 0.005$ (green), $K_1 = 0.01$ (red).

oscillator states. Using the width of the oscillator states and the coupling coefficient, the approximate size of the fluctuations that couple to the qubits will be,

$$\mu_1 \Delta\Phi_{osc} \simeq K_1 \sqrt{2\hbar\omega_{osc} L_{qu}} \sim 1.2 \times 10^{-6} \Phi_0 \qquad (13)$$

for $K_1 = 0.002$ and an oscillator frequency of 100 MHz. The size of the quantum fluctuations that couple across varies linearly with K_1 and as the square root of the frequency. This means that the field frequencies must be very low if strong field-qubit couplings are to be used. Keeping the frequency constant and increasing the oscillator-qubit coupling we find that as soon as the quantum fluctuations become comparable with the constraints on the bias errors, entanglement is effectively lost ($\sim 10^{-5}\Phi_0$ for the cases considered here and $\sim 10^{-6}\Phi_0$ for qubits biased away from the minimum splitting point). Even in the absence of the static bias errors, the quantum noise will affect the generation of entangement between the two qubits. Figure 3 shows the effect of increasing the size of the quantum noise by increasing the coupling to the bias field. For a 100 MHz oscillator and a coupling of $K_1 = 0.01$, giving fluctuations $\mu_1 \Delta\Phi_{osc} \simeq 6 \times 10^{-6}\Phi_0$, the entanglement between the two qubits is lost very quickly. That this is due to quantum fluctuations, rather than the change in coupling strength alone, can be verified by simultaneously changing the oscillator frequency and the coupling strength keeping the size of the quantum noise given by equation (13) fixed.

The quantum fluctuations effectively limit the operating frequency of persistent current qubits as quantum processing devices, because the operating frequency must be lower than the frequency at which the bias fields may be manipulated, which is determined by the frequency

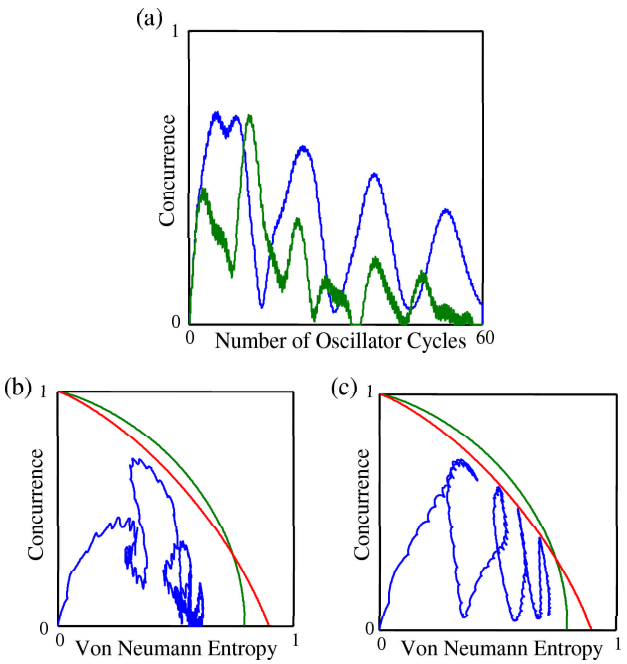

FIG. 4: (a) Concurrence versus number of oscillator cycles (380 MHz) using the quantum model for qubits initialised in the $|0_1 1_2\rangle$ state (blue) and the $|0_1 0_2\rangle$ state (green); (b) Concurrence versus von Neumann entropy for qubits initialised in the $|0_1 0_2\rangle$ state (blue), with two types of maximally entangled mixed states (Rank 3 (green) and Werner states (red) [14]); (c) as (b) for the $|0_1 1_2\rangle$ state.

and the quality factor of the bias circuit. Increasing the operating frequency of the device, and keeping the fluctuations below the required level, would mean reducing the coupling between the qubits and the applied field, which might make it difficult to address individual elements of an array of qubits.

In spite of the possible difficulties in biasing and addressing individual qubits within an array, there are some aspects of the behaviour of this tripartite system that are worth investigating further. In particular, in situations where the frequencies of the oscillator and the qubits are not widely separated, it is possible to generate interesting evolution whereby the currents flowing in the qubits excite oscillations in the bias field, which modifies the behaviour of the qubits. Figure 4 shows examples for a quantum oscillator with a natural frequency of 380 MHz, for both the in-phase and anti-phase initial states (all other parameters are identical to Figure 2). For the $|0_1 0_2\rangle$ initial state, the screening currents flowing in the qubits add in-phase. The net current coupled to the oscillator acts as a sinusoidal drive which excites oscillations in the bias field. In the $|0_1 1_2\rangle$ initial state the net current coupling to the oscillator is close to zero initially and the concurrence oscillations are far more regular. There are significant differences in the concurrence and the von Neumann entanglement between the two cases. In particular, the entanglement persists for longer for the $|0_1 1_2\rangle$ initial state and the von Neumann entropy exhibits some large scale oscillations, as shown by the 'loops' in Figures 4(b) and 4(c). These oscillations in entropy correspond to points where the oscillations in the bias field are at their largest. The oscillations in the field shift the bias point of both of the qubits, which accentuates the natural dephasing between the qubits. As the relative phase of the qubit oscillations changes, the net current coupling to the oscillator changes, and - as they approach the anti-phase state - the net current coupling to the oscillator falls and the oscillations in the field reduce, thereby stabilising the relative phase of the coherent oscillations. Although these phase slips occur for the anti-phase initial state, they are more evident for the in-phase initial state and are responsible for the rapid decay of entanglement in this case and are the dominant source of decoherence.

CONCLUSIONS

In this paper, we have discussed a coupled system consisting of two persistent current qubits and a linear oscillator, representing one of the qubit control fields. We have examined the generation of entanglement between the two qubits in the presence of a dynamical bias field, and have shown that classical models are approximately valid for low frequency fields with high quality factors. We have used the models to set constraints on the accuracy of the applied control fields. The static bias errors must be less than about $5 \times 10^{-5}\Phi_0$ for the parameters used in this paper. We have also considered cases where the underlying quantum fluctuations in the applied field are significant, and have used this to derive a constraint that relates the coupling between the bias field and the qubits and the frequencies present in the bias fields. If these constraints are not met, the useful entanglement between the two qubits is effectively lost. This could affect the use of these devices in a practical quantum processing system, placing severe demands on the accuracy of the static control fields and limiting the operating frequencies of these devices. However, we have found that, where the frequencies of the applied fields and the qubits are comparable, some interesting dynamical behaviour can be produced by the back reaction of the qubits on the applied field.

* Electronic address: jfralph@liv.ac.uk

[1] T.P.Orlando, J.E.Mooji, L.Tian, C.H. van der Wal, L.S.Levitov, S.Lloyd, J.J.Mazo, *Phys. Rev. B* **60**, 15398 (1999).

[2] J.R.Friedman, V.Patel, W.Chen, S.K.Tolpygo, J.E.Lukens, *Nature* **406**, 43 (2000); C.H. van der

Wal, A.C.J. ter Haar, F.K.Wilhem, R.N.Schouten, C.J.P.M.Harmans, T.P.Orlando, S.Lloyd, J.E.Mooij, *Science* **290**, 773 (2000); J.M.Martinis et al. *Phys. Rev. Lett.* **89**, 117901 (2002)

[3] I.Chiorescu, Y.Nakamura, C.J.P.M.Harmans, J.E.Mooij, *Science* **299**, 1869 (2003).

[4] A.J.Berkley,H.Xu, R.C.Ramos, M.A.Gubrud, F.W.Strauch, P.R.Johnson, J.R.Anderson, A.J.Dragt, C.J.Lobb, F.C.Wellstood, *Science* **300**, 1548 (2003); A.Izmalkov, M.Grajcar, E.Il'ichev, Th. Wagner, H.-G.Meyer, A.Yu.Smirnov, M.H.S.Amin, Alec Maassen van den Brink, A.M.Zagoskin, cond-mat/0312332v1, December 2003.

[5] J.F.Ralph, T.P.Spiller, T.D.Clark, R.J.Prance, H.Prance, *Int. J. Mod. Phys. B* **8**, 2637 (1994); J.Diggins, J.F.Ralph, T.D.Clark, T.P.Spiller, R.J.Prance, H.Prance, *Phys. Rev. E* **49**, 1854 (1994); T.D.Clark, J.F.Ralph, R.J.Prance, H.Prance, J.Diggins, R.Whiteman, *Phys. Rev. E* **57**, 4035 (1998).

[6] T.P.Spiller, T.D.Clark, R.J.Prance, H.Prance, *Phys. Lett. A* **170**, 273 (1992).

[7] J.F.Ralph, T.D.Clark, M.J.Everitt, H.Prance, P.Stiffell, R.J.Prance, *Phys. Lett. A* **317**, 199, (2003).

[8] H.J.Carmichael, 'An Open System Approach to Quantum Optics' (Lecture Notes in Physics, Vol.18), Springer-Verlag, Berlin, 1993.

[9] N.Gisin, I.C.Percival, *J. Phys. A* **26**, 2233 (1993); N.Gisin, I.C.Percival, *J. Phys. A* **26**, 2246 (1993); G.C.Hegerfeldt, *Phys. Rev. A* **47**, 449 (1993).

[10] H.M.Wiseman, *Quant. Semiclass. Opt.* **8**, 205 (1996).

[11] M.B.Plenio, P.L.Knight, *Rev. Mod. Phys.* **70**, 101 (1998).

[12] M.Sargent III, M.O.Scully, W.E.Lamb Jr., 'Laser Physics', Ch.16, Addison-Wesley, 1974.

[13] W.K.Wooters, *Phys. Rev. Lett.* **80**, 2245 (1997).

[14] T.-C.Wei, K.Nemoto, P.M.Goldbart, P.G.Kwiat, W.J.Munro, F.Verstraete, *Phys. Rev. A* **67**, 022110 (2003).